Separation of Fine Al_2O_3 Inclusion from Liquid Steel with Super Gravity

CHONG LI, JINTAO GAO, ZHE WANG, and ZHANCHENG GUO

An innovative approach of super gravity was proposed to separate fine Al_2O_3 inclusions from liquid steel in this study. To investigate the removal behaviors of inclusions, the effects of different gravity coefficients and time on separating the inclusions were studied. The results show that a large amount of Al_2O_3 inclusions gathered at the top of the sample obtained by super gravity, whereas there were almost no inclusions appearing at the bottom. The volume fraction and number density of inclusions presented a gradient distribution along the direction of the super gravity, which became steeper with increasing gravity coefficient and separating time. As a result of the collision between inclusions, a large amount of inclusions aggregated and grew during the moving process, which further decreased the removal time. The experimental required removal time of inclusions is close to the theoretical values calculated by Stokes law under gravity coefficient $G \le 80$, $t \le 15$ minutes, and the small deviation may be because the inclusion particles are not truly spherical. Under the condition of gravity coefficient $G = 80$, $t = 15$ minutes, the total oxygen content at the bottom of the sample (position of 5 cm) is only 8.4 ppm, and the removal rate is up to 95.6 pct compared with that under normal gravity.

DOI: 10.1007/s11663-016-0905-5

I. INTRODUCTION

WITH the growth in demand for high-quality steel, the smelting of high-cleanliness steels is becoming increasingly important. And nonmetallic inclusion is one of the important factors affecting the purity of steel, whose presence in steel products has previously been demonstrated to have an adverse influence on the mechanical property,[1] surface quality,[2] fatigue property,[3,4] *etc*. What is worse, it is difficult to remove the micro- and/or nano-sized nonmetallic inclusion from the liquid steel as a result of the fine dispersed distribution. Therefore, effective separation of nonmetallic inclusions is essential for preparing of high-quality steel.

The pursuit of high-cleanliness steels motivates the search for technologies to remove inclusions from liquid steel. The currently used methods within the industry include gas stirring,[5] ceramic filter,[6] bubbling,[7] and electromagnetic purification.[8,9] Generally these methods are effective at removing inclusions of a large size, but the removal efficiency of fine inclusions, particularly those with a similar density to liquid metal, is limited. Therefore, a more effective method for the removal of inclusions of a fine size is strongly desired.

Higee technology, or super gravity, as one of the cutting-edge process intensification technologies, was originally proposed in 1979.[10] Because of its advantages of higher efficiency and free pollution, the applications have been extensively investigated in the chemical process industry[11–13] and electrochemical field.[14,15] In recent years, with the development of technology and the increasing attention paid to super gravity, super-gravity technology has been gradually used to separate the high-temperature melt in the metallurgical field. For example, a phosphorus-enriched phase was successfully enriched and separated by super gravity from a steelmaking slag melt as a result of their density difference.[16] Gao *et al*.[17–20] studied the concentration and separation of valuable elements from different slags by super gravity, and the recovery ratios of valuable elements were pretty remarkable. Zhao *et al*.[21] studied the removal of impurity elements from aluminum melt with super gravity, which make impurity elements Fe and Si segregating at the two ends of the sample along the direction of super gravity, respectively. In addition, Song *et al*.[22] studied the super-gravity separation of nonmetallic inclusions from the aluminum melt, and the effect of super gravity on removal ratio and moving behavior of nonmetallic inclusions was discussed, which proved the feasibility for removal of inclusions in molten metal by super gravity. Inspired by this successful application of super-gravity technology, it would be possible to realize the effective removal of fine inclusions from the liquid steel by super gravity.

In this study, an innovative method of super gravity was introduced to remove the very fine Al_2O_3 nonmetallic inclusions in liquid steel. The effects of super-gravity coefficients and separating time on the microstructure, distribution, and size of nonmetallic inclusions and total oxygen content in a separated sample were investigated. Simultaneously, the removal rate of total oxygen content was further calculated.

CHONG LI, JINTAO GAO, ZHE WANG, and ZHANCHENG GUO are with the State Key Laboratory of Advanced Metallurgy, University of Science and Technology Beijing, 100083 Beijing, P.R. China. Contact e-mail: jintaogao@ustb.edu.cn
Manuscript submitted August 19, 2016.
Article published online January 25, 2017.

II. EXPERIMENTAL

A. *Centrifugal Apparatus*

Figure 1 shows the schematic diagram of the experimental apparatus under a working condition, which is used for super-gravity separation of nonmetallic inclusions from liquid steel. The microwave-absorbing materials inside heat-insulating material can be heated up to 1873 K (1600 °C) by absorbing energy from the microwave generator, and the sample was heated through heat transfer at the same time. The temperature was controlled by a program controller system, which was within the observed precision range of ±3 K (±3 °C) with an R-type thermocouple. Two crucibles with an equal amount of steel were fixed horizontally in the heat-insulating material and symmetrically onto the centrifugal rotor. When the centrifugal system started running, the surface of liquid steel would change from horizontal to vertical and rotate therewith. The gravity coefficient, a ratio of super-gravitational acceleration to gravitational acceleration, was calculated by Eq. [1]:

$$G = \frac{\sqrt{g^2 + (\omega^2 r)^2}}{g} = \frac{\sqrt{g^2 + \left(\frac{N^2\pi^2 r}{900}\right)^2}}{g} \qquad [1]$$

where N is the rotating speed of the centrifugal, r/minute; ω is the angular velocity, rad/second; r is the distance from the centrifugal axis to the sample, 0.11 m; g is normal gravitational acceleration, 9.8 m/s^2. When $N = 0$, G is equal to 1.

B. *Material*

The steel used in this experiment is Al-deoxidized steel taken directly from a ladle, whose chemical composition is shown in Table I.

Without the refining process, the total oxygen content in the steel is up to 381 ppm. Figure 2 shows the type and distribution of nonmetallic inclusion in original steel observed by the scanning electron microscope and energy-dispersive spectrum (SEM-EDS), which indicates that the type of the inclusion was Al_2O_3 presenting a dispersed distribution. The diameter of the most Al_2O_3 inclusion was between 0.2 and 1 μm, which was the size that common refining methods hardly remove from liquid steel.[5–9]

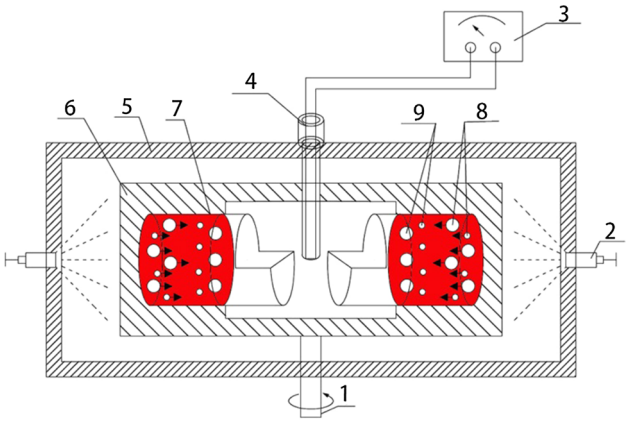

Fig. 1—Schematic diagram of the experimental apparatus under a working condition: 1. centrifugal axis; 2. microwave generator; 3. temperature controller system; 4. thermocouple; 5. heating furnace cavity; 6. heat insulating material; 7. alumina crucible; 8. nonmetallic inclusions before separation; 9. nonmetallic inclusions after separation.

C. *Experimental Procedure and Analysis*

Two Al-deoxidized steel specimens with the same weight of 300 g were separately placed into two alumina crucibles with an inner diameter of 28 mm, which were further put into two graphite crucibles with an inner diameter of 30 mm. Then the two graphite crucibles were fixed horizontally in the heat-insulating material and symmetrically onto the centrifugal rotor. Under the protection of Ar gas at a flow rate of 2 L/minute, the steel was heated to 1853 K (1580 °C) at a rate of 26 K/minute and kept at this temperature for 20 minutes to ensure the steel was in the molten state. And then the centrifugal apparatus was started and adjusted to the specified angular velocity of 400, 600, and 800 rpm; namely, G = 20, 40, or 80 for 1, 5, and 15 minutes, respectively. Afterward, the sample was cooled below the solidification point rapidly and then centrifugal apparatus was shut off and the graphite crucible was taken out. Also, the parallel experiment was carried out for 1 minute in normal gravity (G = 1) for comparison.

One of the two samples obtained by super gravity was sectioned longitudinally along the center axis and then burnished and polished, half of which was used for macro-characterization and the other half was analyzed by SEM-EDS (MLA250) and the automatic inclusion analysis system (EVO18-INCAsteel) to gain the morphology, distribution, size, and type of the nonmetallic inclusion. The other sample was used to analyze the total oxygen content at different positions of 5, 15, and 25 mm along the center axis by an oxygen nitrogen hydrogen analyzer (TCH 600).

III. RESULTS AND DISCUSSION

A. *Macro- and Micro-Characterization of the Samples*

Figure 3 shows cross sections of the sample obtained by super gravity with the gravity coefficient G = 80, temperature T = 1853 K (1580 °C) and time t = 1 minute, compared with the parallel sample under the conditions of gravity coefficient G = 1, temperature T = 1853 K (1580 °C), and time t = 1 minute. As shown in Figure 3(a), the uniform structure presents in the parallel sample without obvious defects under normal gravity, whereas there are significant cracks presenting at the upper part of the sample after super-gravity treatment, as shown in Figure 3(b). To investigate the formation reason of the defects after super gravity further, the microstructure of different positions at the sample, as illustrated in Figures 3(a) through (f), was observed by SEM, and the results were shown in Figure 4. It can be seen from Figure 4(f) that the inclusions in the sample under normal gravity distributed uniformly, whereas those in the sample under super gravity presented gradient distribution

Table I. Chemical Composition of the Used Al-Deoxidized Steel (Mass Fraction, Pct)

Fe	C	Mn	O	N	Si	S	Al
99.02	0.10	<0.10	0.03811	0.00247	<0.10	0.02	0.36

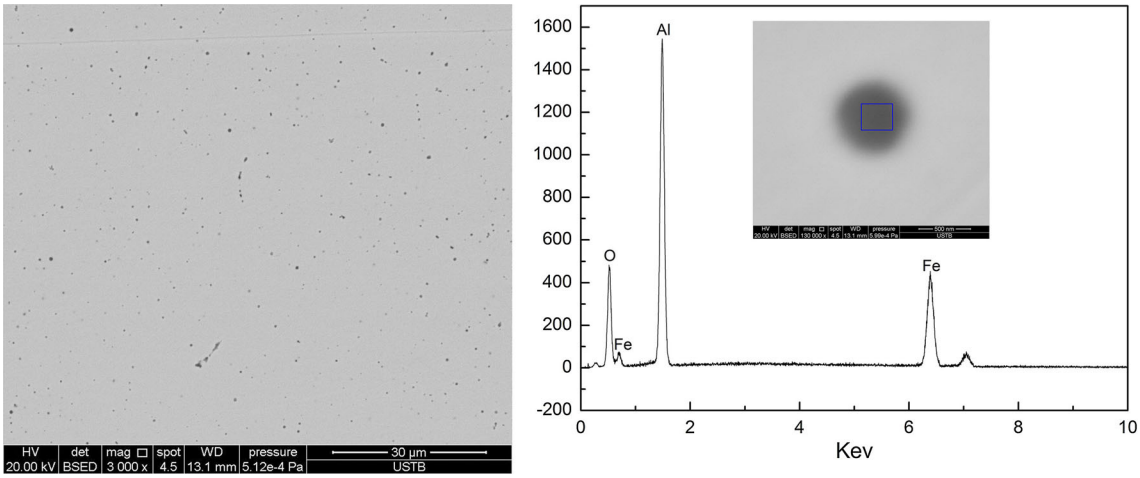

Fig. 2—Type and distribution of inclusion in original steel observed by SEM-EDS.

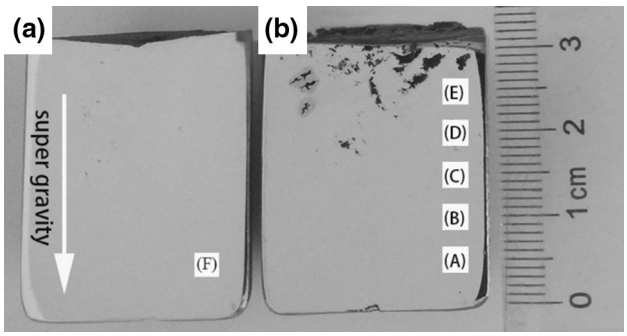

Fig. 3—Macrographs of the samples obtained by super gravity: (*a*) $G = 1$, $t = 1$ min; (*b*) $G = 80$, $t = 1$ min.

along the center axis, as indicated in Figures 4(a) through (e). A large number of inclusions gathered to the upper part of the sample by super gravity at $G = 80$, $T = 1853$ K (1580 °C), $t = 1$ minute, whereas the inclusions could hardly be found at the lower part (Figure 4(a)). Figure 4(e) shows that the inclusions in the upper part existed at two types of dispersion and aggregation, which were both proved to be Al_2O_3 inclusion observed by SEM-EDS, as shown in Figure 5.

Therefore, as described, it is obvious that super gravity has a certain effect on the removal of very fine Al_2O_3 inclusions. In this system, because of the density difference between Al_2O_3 (3.97×10^3 kg m^{-3}) and liquid steel (7.10×10^3 kg m^{-3}), a large amount of inclusions was driven to the top of the sample by super gravity to form a gathering area, which caused the defects of cracks at the upper part of the sample. In comparison, there was no sufficient buoyancy under normal gravity, so the inclusions were still distributed in the sample evenly, which was not enough to cause similar defects during the solidification process of the steel.

B. *Volume Fraction and Number Density Distribution of the Inclusions in the Samples*

To investigate the distributions of the inclusions further, the volume fraction of the inclusions at different distances from the bottom of the sample with different separating time at $G = 80$, $T = 1853$ K (1580 °C) and with different gravity coefficients at $t = 1$ minute, $T = 1853$ K (1580 °C) was counted by an automatic inclusion analysis system, together with the corresponding number density of inclusions at different areas, as shown in Figures 6 and 7. Compared with the parallel sample, the volume fraction and number density of the inclusions presented obvious gradient distribution along the direction of super gravity. As the gravity coefficient and centrifugal time increased, the slope of the gradient distribution became increasingly big. The volume fraction and number density of the inclusions from area (a) to area (c) with the gravity coefficient $G \geq 20$, $t \geq 1$ minutes and $T = 1853$ K (1580 °C) were approaching to zero, obviously less than those with the normal gravity, and then sharply increased toward the top of the samples obtained by centrifugal separation, with the maximum volume fraction and number density of the inclusions appearing in the area (e). The results indicate that a large number of fine Al_2O_3 inclusions, even between 0.2 and 1 μm, could be successfully enriched to the top of the sample with super gravity.

C. *Average Size Distribution and Moving Velocity of the Inclusions in the Samples Under Super Gravity*

Figure 8 presents the variations of the average size of Al_2O_3 inclusions at different areas of the samples with different separating times at $G = 80$, $T = 1853$ K (1580 °C), and different gravity coefficients at $t = 1$ minute, $T = 1853$ K (1580 °C). It can be observed that the average size of the

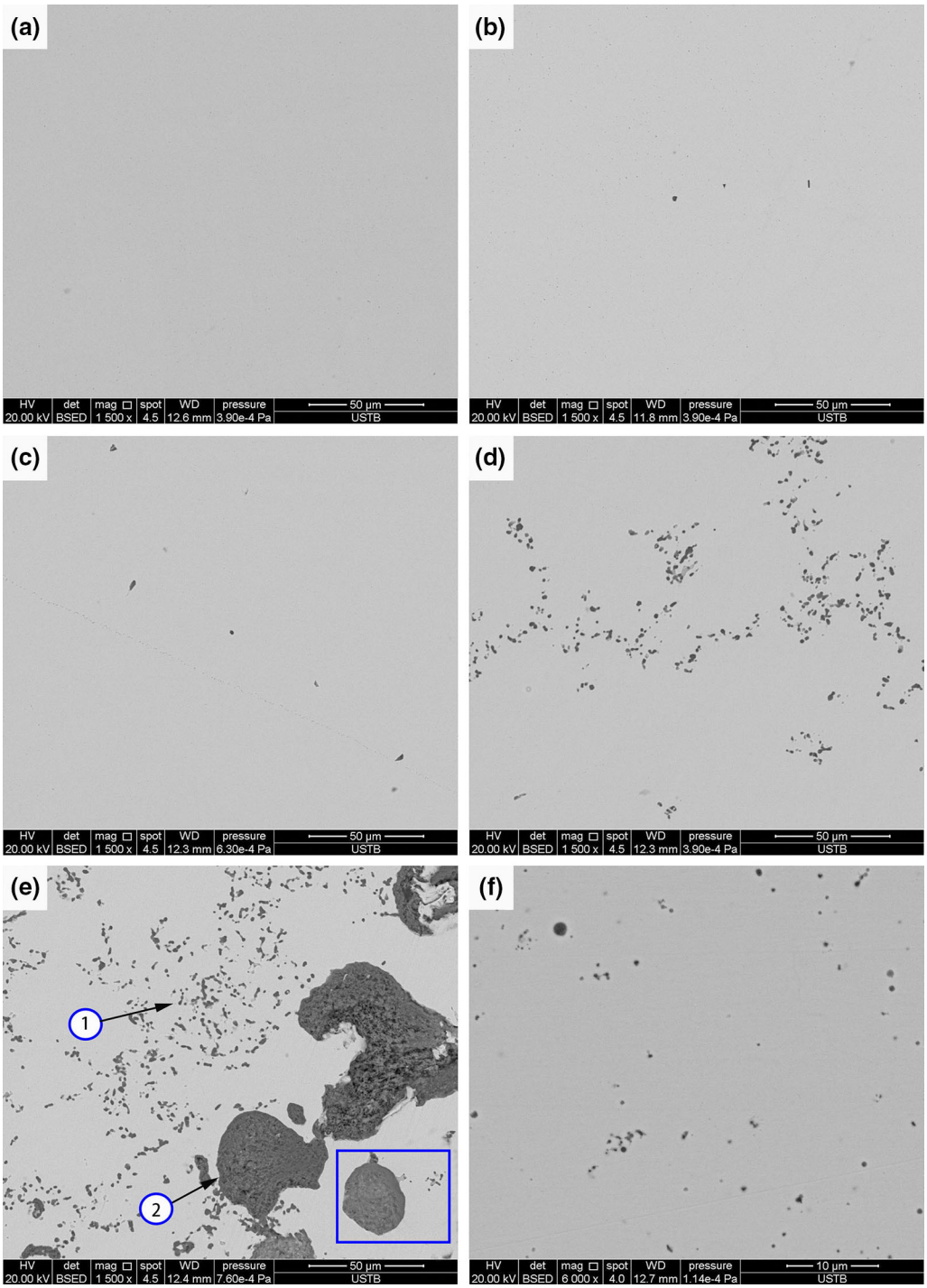

Fig. 4—Micrographs of six areas in the samples obtained by super gravity $G = 80$, $t = 1$ min: ((*a*), (*b*), (*c*), (*d*), (*e*) and (*f*) refer to A, B, C, D, E, and F marked in Fig. 2, respectively).

inclusions in the samples obtained by super gravity was obviously bigger than those in the sample under normal gravity, and the scope was between 0.75 and 5 μm. The average size of the inclusions was gradually distributed in the sample after super gravity, which was obviously bigger at the top of the sample than at the bottom. Simultaneously, the degree of gradient distribution of inclusions was increased when the centrifugal time and gravity coefficient were increased.

It is well known that in a viscous liquid, the velocity of solid particles under a centrifugal force follow Stokes law; when Al_2O_3 inclusions are assumed to be spherical in shape, the motion equation of inclusions in the liquid steel can be calculated by Stokes law.[23,24] It is seen from Eq. [2] that the moving velocity of inclusion under a super-gravity field is proportional to the square of the inclusion diameter

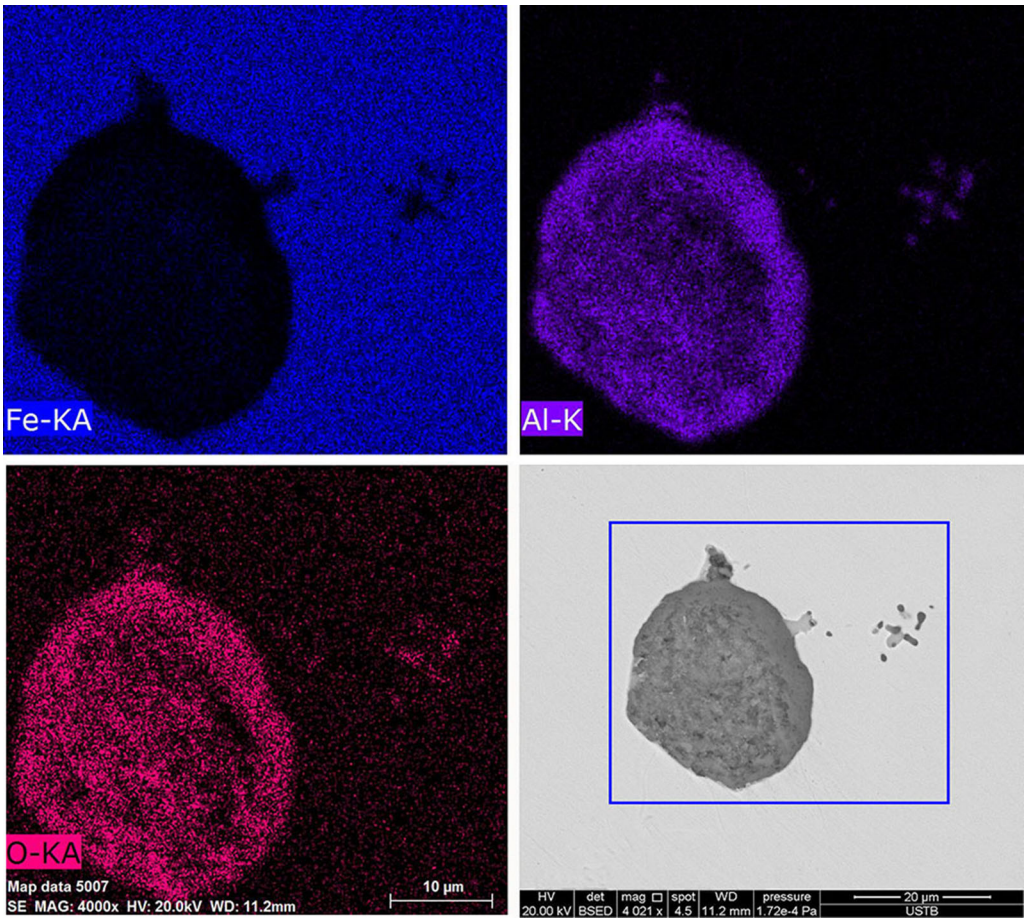

Fig. 5—SEM-mappings of the inclusion in Fig. 4 observed by SEM–EDS.

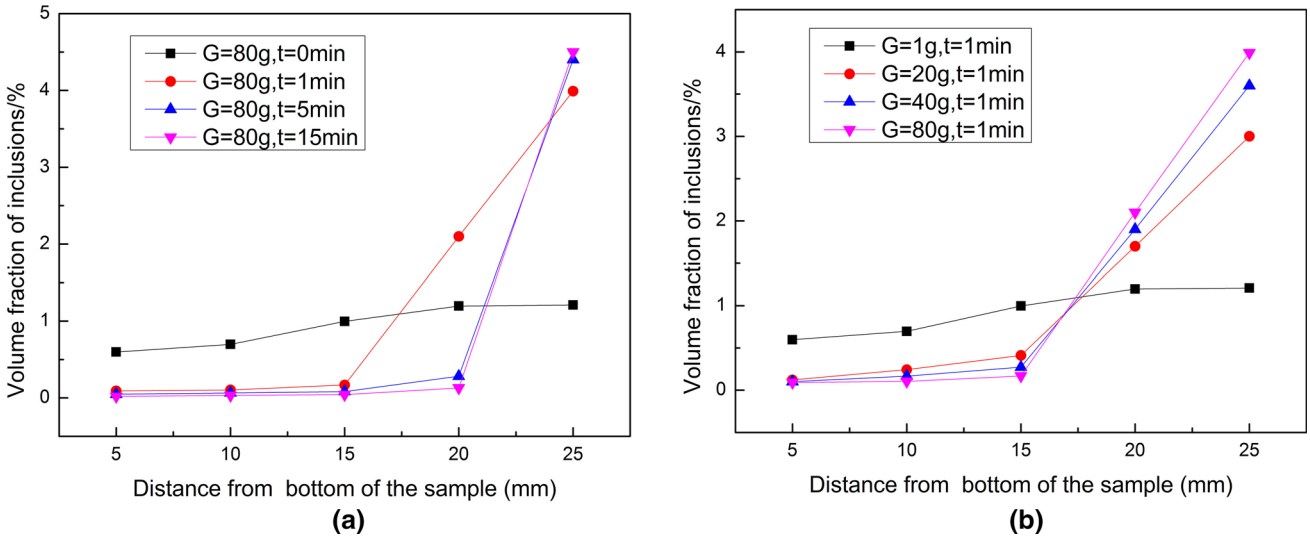

Fig. 6—Volume fraction of inclusions at different distances from bottom of the sample with different conditions: (*a*) $G = 80$, $t = 0$, 1, 5, and 15 min; (*b*) $t = 1$ min, $G = 1$, 20, 40, and 80.

and that large-size inclusion moves faster than the small one, which causes the gradient distribution of inclusions of average size along the direction of super gravity. In addition, the differences in the velocity of inclusions of different diameter will cause the inclusions to collide and grow during the moving process, as discussed by Miki *et al.*,[8] which makes the average size of inclusions increase:

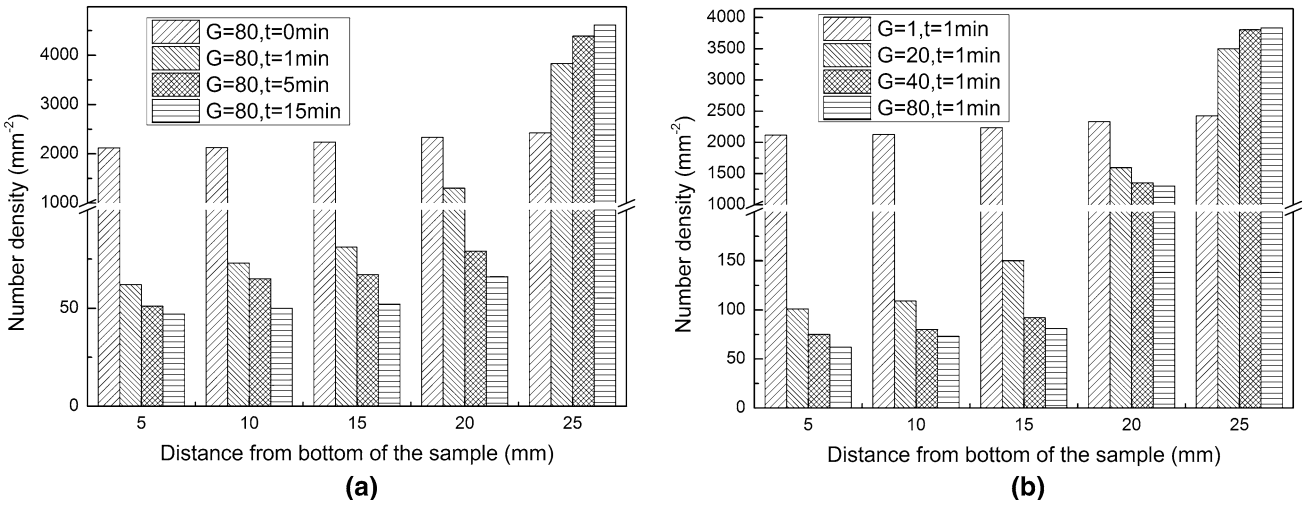

Fig. 7—Number density of inclusions at different distances from the bottom of the sample with different conditions: (*a*) $G = 80$, $t = 0$, 1, 5, and 15 min; (*b*) $t = 1$ min, $G = 1$, 20, 40, and 80.

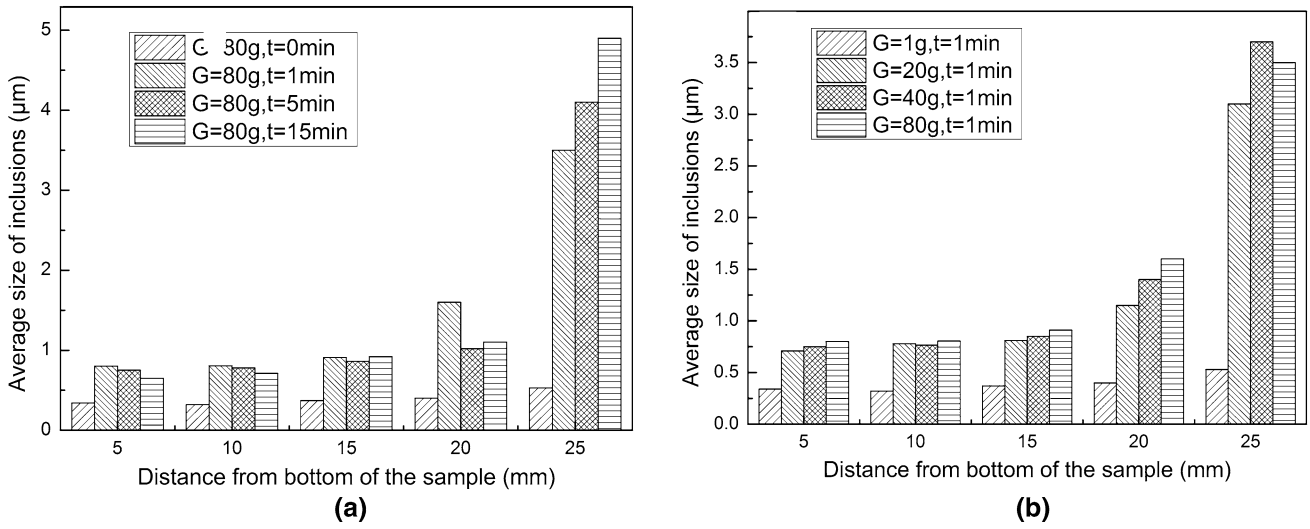

Fig. 8—Average size of inclusions at different distances from the bottom of the sample with different conditions: (*a*) $G = 80$, $t = 0$, 1, 5, and 15 min; (*b*) $t = 1$ min, $G = 1$, 20, 40, and 80.

$$\frac{\mathrm{d}r}{\mathrm{d}t} = \frac{d^2|\rho_\mathrm{L} - \rho_\mathrm{P}|}{18\eta}\omega^2 r \qquad [2]$$

To calculate the required removing time for the inclusions of different sizes from the bottom to the top of the sample, Eq. [2] was further treated as follows:

$$Vr = \frac{d^2\Delta\rho}{18\eta}\omega^2 r \qquad [3]$$

Assuming ω is a constant:[25]

$$r = r' e^{A\omega^2 t} \qquad [4]$$

Thus:

$$t = \frac{1}{A\omega^2}\ln\frac{r}{r\prime} = \frac{900}{A\pi^2 N^2}\ln\frac{r}{r\prime} \qquad [5]$$

where $\mathrm{d}r/\mathrm{d}t$, ρ_L, ρ_P,,ω, r, d, η, and N are motion velocity, the density of liquid, the density of particle, angular velocity, the distance of particle from centrifugal axis, particle diameter, the viscosity of the molten metal, and rotating speed of centrifuge, respectively, and:

$A = \frac{d^2\Delta\rho}{18\eta}$, $\Delta\rho = \rho_\mathrm{L} - \rho_\mathrm{P}$, $Vr = \frac{\mathrm{d}r}{\mathrm{d}t}$

Substituting the density of Al_2O_3 inclusion $\rho_p = 3.97 \times 10^3$ kg m^{-3}, the density of liquid steel $\rho_\mathrm{L} = 7.10 \times 10^3$ kg m^{-3}, the viscosity of liquid steel $\eta = 0.005$ Pa s, $N = 800$ r min^{-1}, $r = 0.11$ m, and $r' = 0.08$ m into Eq. [5]:

$$t = 0.13 \times 10^{-8}\frac{1}{d^2} \qquad [6]$$

Therefore, the required time for the Al_2O_3 inclusions with different sizes moving from the bottom to the top of the sample (3 cm) under gravity coefficient $G = 80$ was calculated by Eq. [6], and the results were shown in Table II. The results show that the theoretical time was

Table II. Required Time of Inclusion Moving From Bottom to Top of the Sample (3 cm) Under Gravity Coefficient $G = 80$

Average size (μm)	0.2	0.5	1	2	3	4	5
Required time (minute)	541.60	86.67	21.67	5.42	2.41	1.35	0.87

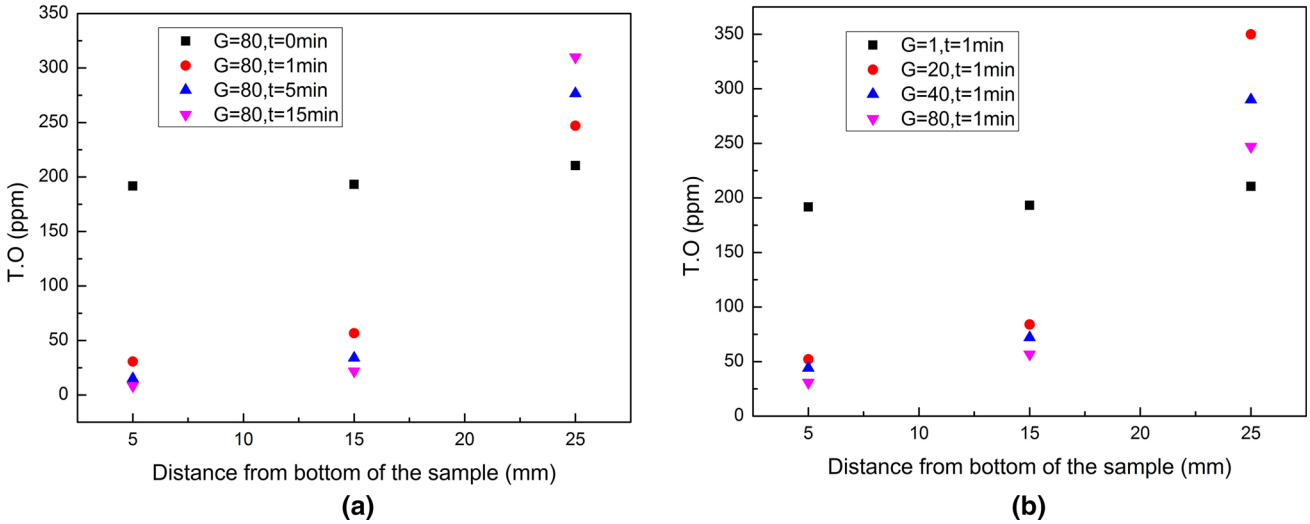

Fig. 9—Total oxygen content of the samples at different distances from the bottom of the sample with different conditions: (*a*) $G = 80$, $t = 0$, 1, 5, and 15 min; (*b*) $t = 1$ min, $G = 1$, 20, 40, and 80.

541.6 minutes for the Al_2O_3 inclusions with the diameter of 0.2 μm moving from the position of 0.11 to 0.08 m under the action of a super-gravity field, whereas it only needs 5.42, 2.51, 1.35, and even 0.87 minutes for the Al_2O_3 inclusions with a diameter of 2, 3, 4, and 5 μm, respectively. It seems impossible to separate these very fine Al_2O_3 inclusions in the Al-deoxidized steel by super-gravity technology; nevertheless, because of the inclusions collision caused by the velocity difference, most inclusions grew up to more than 1 μm under super gravity, as shown in Figures 6 and 8. Therefore, in this experimental study, most inclusions more than 1 μm were driven to the top of the sample at $G = 80$, $t \leq 15$ minutes, and the small ones remained at the lower part. It means that there are good agreements between the experimental and calculated moving velocities, and the small deviation between experimental velocity and calculated theoretical velocity may be because the inclusions are not truly spherical.[26]

D. *Distribution and Removal Rate of Total Oxygen Content in the Samples*

Figure 9 shows the total oxygen content (TO) at different positions of the sample under super gravity and normal gravity. Because a large amount of Al_2O_3 inclusions moved to the top of the sample under super gravity, the TO at the top of the sample after super-gravity separation was more than that in the sample under normal gravity, whereas that at the middle and lower parts of the sample was very small. Just like the volume fraction distribution, the TO in the sample after super gravity presented gradient distribution, too, and the gradient became steeper by increasing the gravity coefficient and centrifugal time. Table III shows the TO and removal rate at the position of 5 mm from the bottom of the sample obtained by different super-gravity coefficients for different separating times.

Table III. Total Oxygen Content and Removal Rate at the Position of 5 mm From the Bottom of the Sample Obtained by Super Gravity

Sample	TO (ppm)	Removal Rate (Pct)
$G = 1$, $t = 1$ minute	191.7	—
$G = 20$, $t = 1$ minute	52.0	72.9
$G = 40$, $t = 1$ minute	44.0	77.0
$G = 80$, $t = 1$ minute	30.7	84.0
$G = 80$, $t = 5$ minutes	15.0	92.2
$G = 80$, $t = 15$ minutes	8.4	95.6

The TO was decreased to 8.4 ppm at the position of 5 mm from the bottom under the conditions of gravity coefficient $G = 80$, $t = 15$ minutes, $T = 1853$ K (1580 °C), and the removal rate of the TO was up to 95.6 pct compared with that under normal gravity, which was calculated *via* Eq. [7]:

$$\varepsilon = \frac{TO_n - TO_s}{TO_n} \times 100\,\text{pct} \qquad [7]$$

where ε is the removal rate, TO_n is the total oxygen content under normal gravity, and TO_s is the total oxygen content under super gravity.

IV. CONCLUSIONS

The removal of very fine Al_2O_3 inclusions from liquid steel under different super-gravity coefficients for different separating times has been investigated in this study. The main conclusions are summarized as follows.

1. The super gravity is proved to be an innovative effective method for removing the very fine Al_2O_3 inclusions from the liquid steel. As a result of the density difference between inclusion and liquid steel, a large amount of inclusions gathered at the top of the sample was obtained by centrifugal separation.
2. The volume fraction and number density of the Al_2O_3 inclusions presented obvious gradient distribution along the direction of super gravity, and the gradient became steeper when increasing the gravity coefficient and centrifugal time.
3. As a result of the collision between inclusions of different velocities under super gravity, a large amount of inclusions aggregated and grew, which theoretically accelerated the removal rate of inclusions from the liquid steel, according to Stokes law. The study indicates that the experimental moving velocities of inclusions were close to the theoretical moving velocities obtained by Stokes law under gravity coefficient $G \leq 80$, $t \leq 15$ minutes, and the small deviation might be because the inclusions were not truly spherical.
4. The total oxygen content at the bottom of the sample obtained by super gravity $G = 80, t = 15$ minutes, was only 8.4 ppm, and the removal rate was up to 95.6 pct when compared with that under normal gravity.

ACKNOWLEDGMENT

This work is supported by the National Natural Science Foundations of China (Nos. 51234001 and 51404025) and the Fundamental Research Funds for the Central Universities (FRF-TP-15-009A2), which is acknowledged with thanks.

REFERENCES

1. S. Liu, Q. Huang, C. Li, and B. Huang: *Fusion Eng. Des.*, 2009, vol. 84, pp. 1214–18.
2. K. Shiozawa, Y. Morii, S. Nishino, and L. Lu: *J. Soc. Mater. Sci. Jpn.*, 2003, vol. 52, pp. 1311–17.
3. Z.G. Yang, J.M. Zhang, S.X. Li, G.Y. Li, Q.Y. Wang, W.J. Hui, and Y.Q. Weng: *Mater. Sci. Eng. A*, 2006, vol. 427, pp. 167–74.
4. G. Qian, Y. Hong, and C. Zhou: *Eng. Fail. Anal.*, 2010, vol. 17, pp. 1517–25.
5. L.T. Wang, Q.Y. Zhang, S.H. Peng, and Z.B. Li: *ISIJ Int.*, 2005, vol. 45, pp. 331–37.
6. Z. Taslicukur, C. Balaban, and N. Kuskonmaz: *J. Eur. Ceram. Soc.*, 2007, vol. 27, pp. 637–40.
7. L. Zhang and S. Taniguchi: *Int. Mater. Rev.*, 2000, vol. 45, pp. 59–82.
8. Y. Miki, H. Kitaoka, T. Sakuraya, and T. Fujii: *ISIJ Int.*, 1992, vol. 32, pp. 142–49.
9. Y. Miki, S. Ogura, and T. Fujii: *Kawasaki Steel Technical Report-English Edition*, 1996, pp. 67–73.
10. C. Ramshaw and R.H. Mallinson: Patent 0002568, 1979.
11. A. Das, A. Bhowal, and S. Datta: *Ind. Eng. Chem. Res.*, 2008, vol. 47, pp. 4230–35.
12. C.C. Lin and K.S. Chien: *Separ. Purif. Tech.*, 2008, vol. 63, pp. 138–44.
13. Y.S. Chen, F.Y. Lin, C.C. Lin, C.Y.D. Tai, and H.S. Liu: *Ind. Eng. Chem. Res.*, 2006, vol. 45, pp. 6846–53.
14. T. Liu, Z.C. Guo, Z. Wang, and M.Y. Wang: *Appl. Surf. Sci.*, 2010, vol. 256, pp. 6634–40.
15. M.Y. Wang, Z. Wang, Z.C. Guo, and Z.J. Li: *Int. J. Hydro. Energy*, 2011, vol. 36, pp. 3305–12.
16. C. Li, J.T. Gao, and Z.C. Guo: *Metall. Mater. Trans. B*, 2016, vol. 47B, pp. 1516–19.
17. J.T. Gao, Y.W. Zhong, and Z.C. Guo: *Metall. Mater. Trans. B*, 2016, vol. 47B, pp. 2459–67.
18. J.T. Gao, Y.W. Zhong, L. Guo, and Z.C. Guo: *Metall. Mater. Trans. B*, 2016, vol. 47B, pp. 1080–92.
19. J.T. Gao, Y.W. Zhong, and Z.C. Guo: *ISIJ Int.*, 2016, vol. 56, pp. 1352–57.
20. J.T. Gao, L. Guo, and Z.C. Guo: *ISIJ Int.*, 2015, vol. 55, pp. 2535–42.
21. L.X. Zhao, Z.C. Guo, Z. Wang, and M.Y. Wang: *Metall. Mater. Trans. B*, 2010, vol. 41B, pp. 505–08.
22. G.Y. Song, B. Song, Y.H. Yang, Z.B. Yang, and W.B. Xin: *Metall. Mater. Trans. B*, 2015, vol. 46B, pp. 2190–97.
23. Y. Watanabe, A. Kawamoto, and K. Matsuda: *Compos. Sci. Tech.*, 2002, vol. 62, pp. 881–88.
24. Y. Watanabe, Y. Inaguma, H. Sato, and E. Miura-Fujiwara: *Materials*, 2009, vol. 2, pp. 2510–25.
25. J.C. Li, Z.C. Guo, and J.T. Gao: *ISIJ Int.*, 2014, vol. 54, pp. 743–49.
26. S.G. Shabestari and J.E. Gruzleski: *Metall. Mater. Trans. A*, 1995, vol. 26A, pp. 999–1006.